

## Efficient Cellular Labeling by CD44 Receptor-Mediated Uptake of Cationic Liposomes Functionalized with Hyaluronic Acid and Loaded with MRI Contrast Agents

Giovanna Esposito, Simonetta Geninatti Crich, and Silvio Aime<sup>\*[a]</sup>

Cell tracking is now a well-established technique in magnetic resonance imaging (MRI) because of its three-dimensional capabilities, its good safety profile, and the superb anatomical resolution (near the cellular level,  $\sim 100 \mu\text{m}$ ).<sup>[1–4]</sup> For these applications, cells must be labeled with MRI contrast agents in order to decrease the relaxation times of the H atoms of water molecules. The most common contrast agents in current use are iron oxide particles (USPIO, SPIO, MPIO) because of their high sensitivity. They act as negative contrast agents because of their dominant effect on the magnetic susceptibility term.<sup>[5,6]</sup> Typically the  $R_2$  value of monocytes labeled with SPIO at a Fe concentration of  $1.0 \text{ mg mL}^{-1}$  is  $13.1 \text{ s}^{-1} \text{ mm}^{-1}$ . It has been shown that this leads to a detection limit of 58 labeled monocytes per voxel volume of  $0.05 \text{ mL}$ .<sup>[7]</sup> These magnetic particles enable the visualization of labeled cells as dark spots in the MR images as a consequence of their largely dominant  $T_2^*$  effects. However, there is some concern about their long-term cellular toxicity related to the metabolic fate of the iron payload.<sup>[8,9]</sup> Other problems with superparamagnetic particles include difficulty in the quantification of cell number due to susceptibility artifacts and the potential transfer of contrast among cells (macrophages) after cell death, giving false-positive results.<sup>[10]</sup>

The use of positive contrast agents is a viable alternative to overcome these problems, but to attain sufficient contrast for the MRI of the labeled cells, it is necessary to entrap a number of Gd complexes on the order of  $10^7$ – $10^8$  per cell.<sup>[12]</sup> Various routes have been explored in pursuit of effecting the internalization of such large quantities of paramagnetic complexes. Pinocytosis is sometimes a useful route, but the cells must be kept in the presence of high concentrations ( $\sim 50 \text{ mM}$ ) of highly stable, hydrophilic agents for many hours (12–24 h).<sup>[12,13]</sup> Rapid entrapment of the required Gd complexes may be attained by electroporation of the cell suspension;<sup>[14]</sup> however, this treatment results in extensive cell death and serious damage to surviving cells. Finally, for cells endowed with phagocytic activity, it has been shown that cellular labeling can be achieved by using particles made of insoluble Gd complexes.<sup>[11,15]</sup> These particles are designed to be solubilized upon release of insolubilizing moieties effected by a specific enzyme present in the cellular compartment in which these particles have been entrapped. This procedure is particularly efficient,

as it allows the entrapment of a large number of Gd complexes through a single internalization step.

Herein we report a cellular labeling methodology that allows the rapid internalization of large amounts of soluble Gd complexes through exploitation of the receptor-mediated endocytotic route. The Gd<sup>3+</sup> payload is contained in the inner cavity of liposomes, which are appropriately functionalized at their external surface to bind a given receptor, thus starting the uptake process.

As a proof of concept, hyaluronan (hyaluronic acid, HA) was used as a vector for the targeting procedure because HA receptors (CD44) are expressed in a variety of tumors such as breast, colon, intestinal, and brain, as well as melanoma, basal cell carcinoma, and stem cells.<sup>[16–18]</sup>

HA is a high-molecular-weight glycosaminoglycan polymer ( $M_r$ :  $10^6$ – $10^7$  Da) composed of repeating units of the disaccharide  $\beta$ 1,3-*N*-acetylglucosaminyl- $\beta$ 1,4-glucuronide. Thus each disaccharide moiety contains a free carboxylate group, leading to highly negatively charged polymer. For the purpose of this application, HA can be bound to the surface of Gd-loaded liposomes in either a covalent<sup>[16]</sup> or noncovalent manner.<sup>[19]</sup> The formation of a noncovalent supramolecular adduct appeared a straightforward route, as cationic liposomes have been widely used in transfection experiments as carriers of negatively charged DNA macromolecules.<sup>[20,21]</sup>

Cationic liposomes were prepared by using a mixture of phospholipids (POPC 52% and DOTAP 25%) and cholesterol (23%). The lipid film was hydrated with an aqueous solution of Gd-HPDO3A (100 mM). The latter is a commercially available, highly hydrophilic, neutral MRI contrast agent largely used in clinical practice. The liposomes thus formed were extruded through progressively smaller pore sizes to select a population with an average diameter of  $127 \pm 5 \text{ nm}$  and a  $\zeta$  potential of  $+35 \pm 5 \text{ mV}$ . The Gd complexes not entrapped in the liposomes were removed by dialysis. The supramolecular HA-functionalized Gd-liposome (HA-L) adducts were obtained by adding aliquots of a solution of HA to the liposome suspension. Interestingly, a dramatic increase in the supramolecular adduct size takes place (Figure 1a) at the isoelectric point—the point at which the number of positive charges on the liposome equals the number of negative charges on the added HA polymer. Light scattering measurements showed that the particle diameter nearly triples ( $\sim 350 \text{ nm}$ ) under these conditions, suggesting the formation of an aggregate that consists of three to four liposomes and several HA molecules (Scheme 1). At higher HA/liposome stoichiometric ratios, the prevalence of a monomeric liposome population was again detected. It appears that in the presence of an excess in positive

[a] Dr. G. Esposito, Dr. S. Geninatti Crich, Prof. S. Aime  
Dipartimento di Chimica IFM and Molecular Imaging Center  
Via Nizza 52, 10125 Torino (Italy)  
Fax: (+39) 011-670-6487  
E-mail: silvio.unito@unito.it

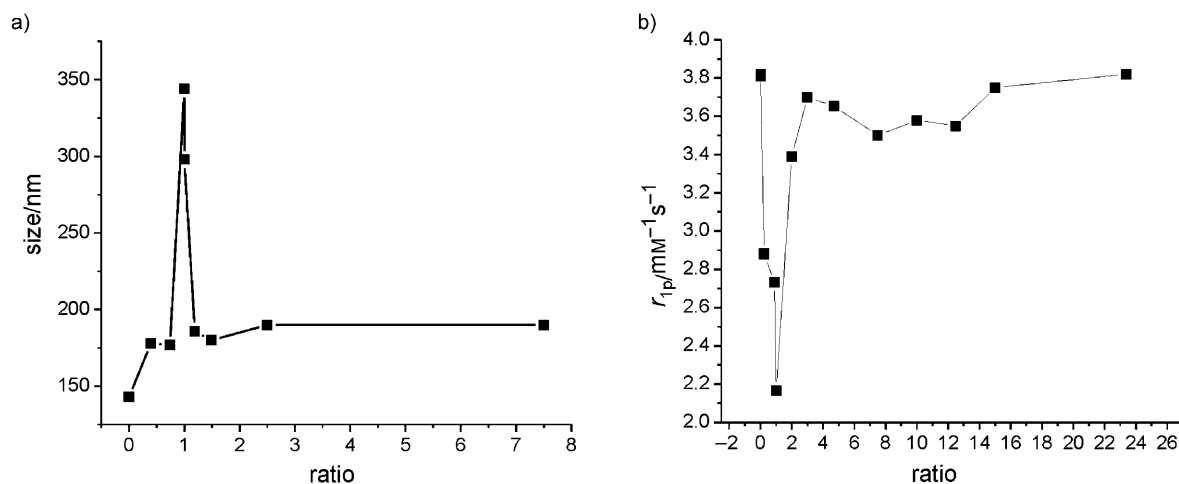
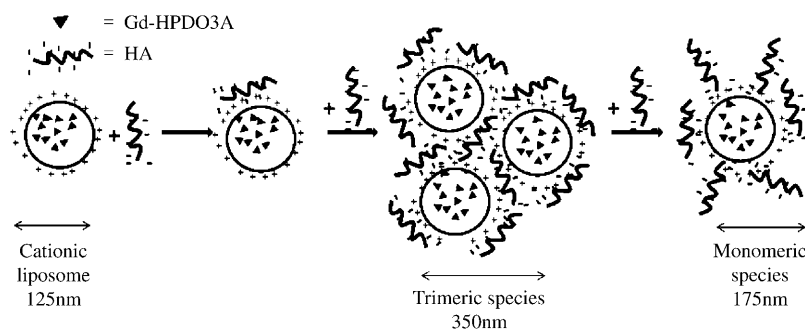


**Figure 1.** Distribution of a) size and b) relaxivity of HA-functionalized Gd-liposomes (HA-L) obtained from mixing a suspension of cationic liposomes ( $50 \mu\text{g mL}^{-1}$  lipids) with increasing amounts of HA at  $25^\circ\text{C}$  for 5 min; ratio = mol negative charges over positive charges.



**Scheme 1.** Schematic representation of HA-liposome interactions. Large-sized adducts are formed when the stoichiometric ratio between positive (brought by liposomes) and negative (brought by HA) charges are close to unity.

or negative charge, electrostatic repulsion prevents extensive aggregation, thus favoring the formation of smaller adducts. In contrast, the formation of large adducts is favored in the case of overall charge-neutral HA-L adducts, for which electrostatic repulsion is minimal.

The composition of the liposome membrane is highly water permeable. In fact, the observed relaxivity ( $r_{1p}$ ) of Gd-HPDO3A entrapped in the cationic liposome cavity is only 10% lower than the free complex, that is, 3.8 versus  $4.2 \text{ mm}^{-1}\text{s}^{-1}$  (20 MHz,  $25^\circ\text{C}$ ), respectively. The addition of HA at the outer surface affects water permeability only when the large-size aggregates are formed, as shown by the marked decrease in  $r_{1p}$  when the positive charges of the liposome are neutralized by the negative charges of the HA polymer (Figure 1b). The formation of the large-size aggregates likely decreases the surface area of liposomes in contact with the aqueous phase, thus decreasing the overall exchange of water molecules between the outer and inner compartments of liposomes, resulting in a net decrease of  $r_{1p}$  (down to  $2.15 \text{ mm}^{-1}\text{s}^{-1}$ ). At higher HA/liposome ratios the occurrence of monomeric liposome species causes the recovery of the initial relaxation rate. Thus, avoiding the neutral adduct, the overall characteristics of membrane perme-

ability of these HA-functionalized Gd-liposomes are such that the diffusion of water molecules occurs almost freely at the NMR time scale.

The capacity of these HA-L adducts in targeting CD44 receptors was explored with three tumor cell types (C6 rat glioma, B16-F10 mice melanoma, and MCF7 human breast cancer) that have varied CD44 receptor expression levels.<sup>[16,22,23]</sup> Cells ( $\sim 1.5 \times 10^6$ ) were incubated in medium containing HA-L (HA/

liposome = 4:1, the ratio of which is defined by moles of negative/positive charge), or nonfunctionalized Gd-loaded liposomes (L) for 30 min. In both experiments the Gd concentration in the incubation medium was  $0.01 \text{ mM}$ .

As shown in Figure 2b, despite the low concentration of HA-L used, good MRI of C6 and B16-F10 cells was obtained. The MRI signal enhancement is directly proportional to the expression level of CD44 receptors (C6 > B16-F10 > MCF7), as independently measured by fluorimetric cytometry (data not shown).

Based on these results, a more detailed study of HA-L internalization in C6 cells was carried out. Figure 3a and 3b shows the amount of Gd entrapped in C6 cells upon incubation in the presence of HA-L or L at various times and concentrations. The cells were observed to rapidly internalize HA-L, and uptake saturation is quickly reached. This behavior appears to derive from saturation of the uptake system rather than depletion of HA-L, as the liposome concentration in the medium decreases by only 12% over the course of incubation. The uptake of L was linear with its concentration in the incubation medium, as expected for internalization through nonspecific binding. To reach the same amount of Gd as in the case of

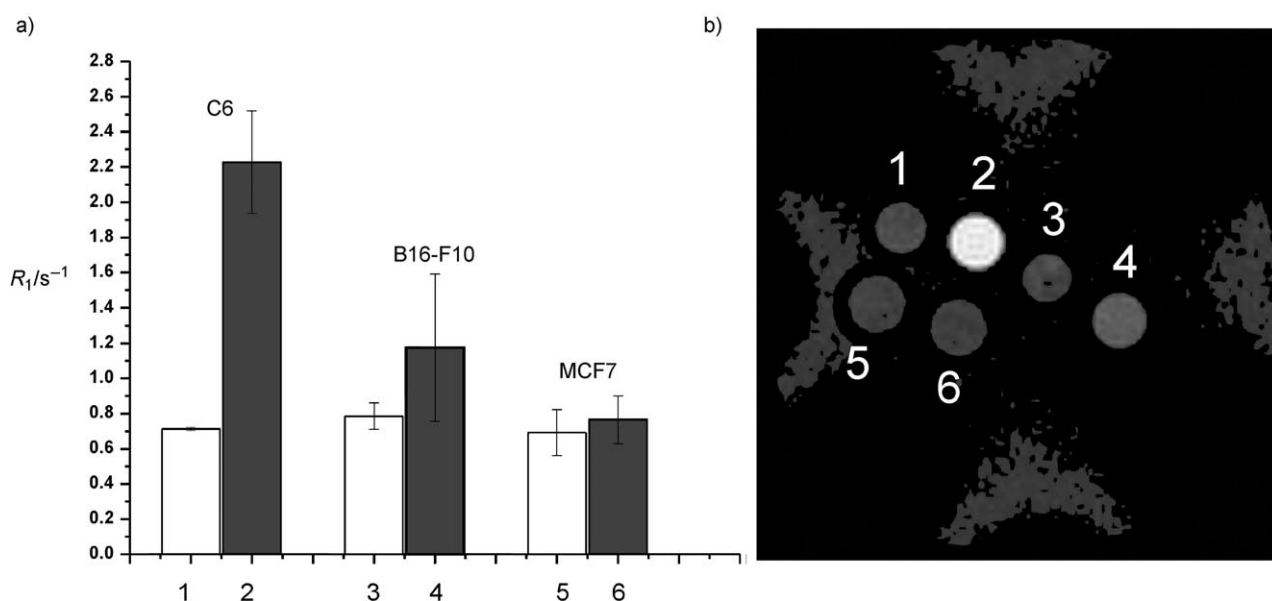


**Figure 2.** a)  $^1\text{H}$  relaxation rates of C6 (1,2), B16-F10 (3,4), and MCF-7 (5,6) cellular pellets after incubation at  $37^\circ\text{C}$  for 30 min in the presence of L (white bar) and HA-L with a fourfold excess of negative charges (dark bar). In both experiments the concentration of Gd is 0.01 mM. b) Corresponding  $T_1$ -weighted MR image of a phantom containing cellular pellets after incubation in the presence of L (1,3,5) or HA-L (2,4,6); the C6 pellet from the incubation with HA-L (2) is particularly intense.

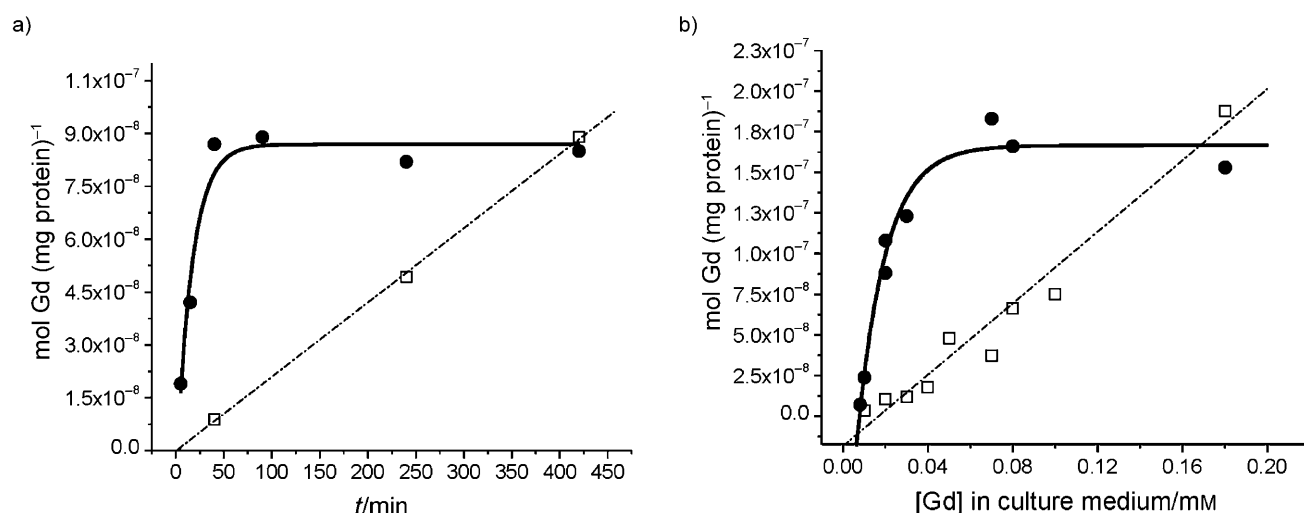


**Figure 3.** Internalization of HA-L (●) and L (□) in C6 cells. a)  $1.5 \times 10^6$  cells were incubated at  $37^\circ\text{C}$  with L and HA-L ( $[\text{Gd}] = 0.02$  mM) at various times. b)  $1.5 \times 10^6$  cells were incubated at  $37^\circ\text{C}$  for 30 min in the presence of increasing concentrations of L and HA-L.

HA-L, the concentration must be four- to fivefold greater. Conversely, the observed isotherm shown by HA-L clearly indicates a specific saturation that would occur through CD44 receptor-mediated uptake.

Moreover, upon comparison of the observed relaxation of the cellular pellets as a function of intracellular concentration (Figure 4), one may confirm that the Gd complexes internalized through the CD44 receptor route follow an endosomal compartmentalization.<sup>[16]</sup> In fact, whereas the cytoplasmic distribution leads to a linear relationship between the observed relaxation rate and the intracellular Gd content, the endosomal localization limits such a relationship up to only  $\sim 7 \times 10^{-8}$  mol Gd

per mg protein (i.e.  $\sim 2.5 \times 10^9$  Gd ions per cell). The relaxation data obtained herein for HA-L and L (Figure 4) agree very well with the previously reported result for Gd-HPDO3A internalized into endosomes by pinocytosis.<sup>[14]</sup>

The uptake of the supramolecular adduct HA-L prepared at the isoelectric point (HA/liposome charge ratio = 1:1) was also investigated. C6 cells were incubated for 30 min at  $37^\circ\text{C}$  with increasing concentrations of HA-L (0.01–0.07 mM), and a slight increase in Gd uptake of  $\sim 25\%$  was detected with respect to the HA/liposome adduct used above, corresponding to a system in which the negative charges are in fourfold excess over positive charges.

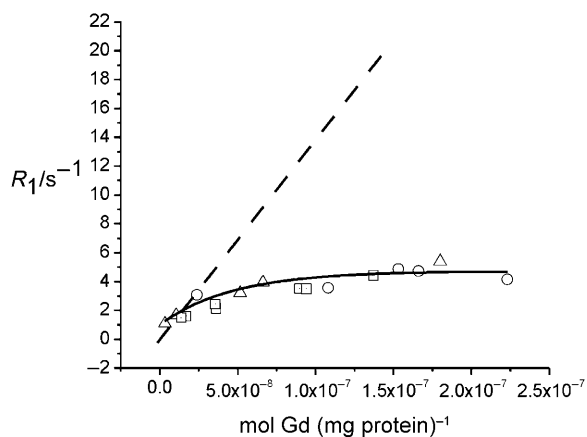


**Figure 4.** Water proton longitudinal relaxation rates of C6 cells labeled with HA-L (○), L (△), and Gd-HPDO3A (□). The dashed line represents the linear relationship previously reported for uptake by electroporation, whereas the solid curve follows the hyperbolic behavior of pinocytotic uptake.

The viability of C6 cells incubated in the presence of L and HA-L, as evaluated by trypan blue assay, was > 98%. We therefore conclude that the HA-L adduct is nontoxic at all concentrations investigated.

Finally, the time-dependent release of Gd chelates from labeled C6 cells was investigated. Cultured C6 cells double their numbers daily. Therefore the contrast attainable decreases according to the number of cell divisions. Cells labeled with HA-L showed a decrease in the relaxation rate from 5.2 to 0.8 s<sup>-1</sup> over the course of ~72 h, reflecting three cell divisions. This decrease in relaxivity is determined by the decrease in the amount of Gd per cell as a result of cell division. In determining the Gd content of each specimen, it was found that the number of Gd ions per cell decreases from 5.3 × 10<sup>9</sup> to 1.2 × 10<sup>9</sup>. During this time, the total amount of Gd entrapped in the cells changed from ~4 × 10<sup>15</sup> to 3 × 10<sup>15</sup>, corresponding to a decrease of 31%. Thus only about one third of the endosome-internalized Gd, in the form of Gd-loaded liposomes, is released into the culture medium over a three-day period. This is likely associated with an exocytosis process during cellular division. This is an important observation in the development of new labeling methods that are designed to detect grafted cells many days after transplantation.

In summary, the results reported herein show that receptor-mediated endocytosis is an efficient route for cell labeling. HA-L shows a very good affinity for cells, such as the C6 line, that express high levels of the CD44 receptor. Thanks to simple electrostatic interactions, it is possible to produce an efficient and specific contrast agent for MRI that allows rapid and reliable cell labeling with minimal toxicity. This method represents one of the most efficient MRI labeling procedures so far reported, in application to CD44 targeting. This technique may be extended to several other targets through the proper choice of liposomes and vector moieties. Moreover, liposomes may be loaded with drugs, thus allowing the interesting perspective of visualizing therapeutic treatments by drug delivery through cellular carriers.

## Experimental Section

Gd-HPDO3A (Prohance) was kindly provided by Bracco Imaging S.p.A. All other chemicals were purchased from Sigma-Aldrich (St. Louis, MO, USA). Cationic liposomes were obtained by hydrating a thin-layer mixture of phospholipids/cholesterol (POPC/DOTAP 2.26:1 molar ratio; POPC = 1-palmitoyl-2-oleoyl-*sn*-glycero-3-phosphocholine, DOTAP = 1,2-dioleoyl-3-trimethylammonium propane) with an aqueous solution of the neutral complex Gd-HPDO3A (100 mM; HPDO3A = 1,4,7,10-tetraazacyclododecane-1-hydroxymethylpropyl-4,7,10-triacetic acid). The suspension was then extruded four times on polycarbonate filters of 400 nm and then four times on polycarbonate filters of 200 nm (Northern Lipids, USA). The resulting unilamellar vesicles were extensively purified by dialysis against a buffer solution (HEPES 5 mM, NaCl 0.15 M, pH 7.4). The size and  $\zeta$  potential were measured by dynamic light scattering on a Malvern Zetasizer Nano ZS instrument (Malvern, UK). The longitudinal water proton relaxation rate of cationic liposomes was measured on a Stellar Spinmaster spectrometer (Stellar, Mede, Italy) operating at 20 MHz.

Cell labeling was carried out on rat glioma (C6), mouse melanoma (B16-F10) and human breast cancer cells (MCF7) obtained from the American Type Culture Collection. Cells were grown in culture flasks (75-cm<sup>2</sup>): C6 in DMEM-F12 supplemented with 5% fetal bovine serum (FBS), B16-F10 in RPMI 1640 with 4.5 g L<sup>-1</sup> glucose and 10% FBS, and MCF7 in DMEM with 10% FBS. All media were supplemented with glutamine (2 mM), penicillin (100 U mL<sup>-1</sup>), and streptomycin (100  $\mu$ g mL<sup>-1</sup>). For in vitro uptake experiments, ~4.5 × 10<sup>5</sup> cells were seeded in culture dishes ( $\varnothing$  = 6 cm). Two days later, cells were incubated with L or HA-L at 37 °C for 30 min in a humidified atmosphere of 5% CO<sub>2</sub>, and were then washed three times with phosphate-buffered saline and subsequently harvested with a solution of trypsin/EDTA. The trypan blue exclusion test was used to assess cell viability.

All MR images were acquired on a Bruker Avance 300 spectrometer (7T) equipped with a Micro 2.5 microimaging probe (Bruker Bio-Spin, Milan, Italy). The glass capillaries containing ~1.5 × 10<sup>6</sup> cells were placed in an agar phantom, and MR imaging was performed using a standard T<sub>1</sub>-weighted multislice multiecho sequence (TR/TE/NEX = 200:3.3:16, FOV = 1.2 cm, one slice = 1 mm, in-plane resolution = 94 × 94  $\mu$ m). The T<sub>1</sub> measurement of cell pellets was performed by using a saturation recovery sequence.

Gd content in the cell pellet was determined using inductively coupled plasma mass spectrometry (ICP-MS) (Element-2, Thermo-Finnigan, Rodano (MI), Italy). Sample digestion was performed with 2 mL concentrated HNO<sub>3</sub> (70%) under microwave heating (Milestone MicroSYNTH Microwave Labstation equipped with an optical fiber temperature control and HPR-1000/6M six-position high-pressure reactor, Bergamo, Italy). After digestion, the volume of each sample was brought to 2 mL with ultrapure water, and the sample was analyzed by ICP-MS. Three replicates of each sample solution were analyzed. The protein concentration of each sample was determined from cell lysates by the Bradford method using bovine serum albumin as standard; 1 mg protein corresponds to ~14 × 10<sup>6</sup> C6 cells.

## Acknowledgements

This work was supported by MIUR (FIRB project), Encite, Meditrans IP, Emil, and DiMI EU NoEs. Support from Bracco Imaging S.p.A. is gratefully acknowledged.

**Keywords:** cationic liposomes • CD44 • contrast agents • hyaluronic acid • molecular imaging

- [1] M. Hoehn, D. Wiedermann, C. Justicia, P. R. Cabrer, K. Kruttwig, T. Farr, U. Himmelreich, *J. Physiol.* **2007**, *584*, 25–30.
- [2] B. Gimi, D. Artemov, T. Leong, D. H. Gracias, W. Gilson, M. Stuber, Z. M. Bhujwala, *Cell Transplant.* **2007**, *16*, 403–408.
- [3] A. S. Krishnan, A. A. Neves, M. M. de Backer, D. E. Hu, B. Davletov, M. I. Kettunen, K. M. Brindle, *Radiol.* **2008**, *246*, 854–862.
- [4] M. Modo, M. Hoehn, J. W. Bulte, *Mol. Imaging* **2005**, *4*, 143–164.
- [5] S. A. Anderson, K. K. Lee, J. A. Frank, *Invest. Radiol.* **2006**, *41*, 332–338.
- [6] J. W. Bulte, D. L. Kraitchman, *NMR Biomed.* **2004**, *17*, 484–499.
- [7] R. D. Oude Engberink, S. M. van der Pol, E. A. Dopp, H. E. de Vries, E. L. Blezer, *Radiol.* **2007**, *243*, 467–474.
- [8] T. R. Pisanic, J. D. Blackwell, V. I. Shubayev, R. R. Fiñones, S. Jin, *Biomaterials* **2007**, *28*, 2572–2581.
- [9] E. Farrell, P. Wielopolski, P. Pavljasevic, S. van Tiel, H. Jahr, J. Verhaar, H. Weinans, G. Krestin, F. J. O'Brien, G. van Osch, M. Bernsen, *Biochem. Biophys. Res. Commun.* **2008**, *369*, 1076–1081.
- [10] K. Hoshino, H. Q. Ly, J. V. Frangioni, R. J. Hajjar, *Prog. Cardiovasc. Dis.* **2007**, *49*, 414–420.
- [11] S. Aime, C. Cabella, S. Colombatto, S. Geninatti Crich, E. Gianolio, F. Maggioni, *J. Magn. Reson.* **2002**, *16*, 394–406.
- [12] S. Geninatti Crich, L. Biancone, V. Cantaluppi, D. Duó, V. Cantaluppi, G. Esposito, S. Russo, G. Camussi, S. Aime, *Magn. Reson. Med.* **2004**, *51*, 938–944.
- [13] L. Biancone, S. Geninatti Crich, V. Cantaluppi, G. M. Romanazzi, S. Russo, E. Scalabrino, G. Esposito, F. Figliolini, S. Beltramo, P. C. Perin, G. P. Segoloni, S. Aime, G. Camussi, *NMR Biomed.* **2007**, *20*, 40–48.
- [14] E. Terreno, S. Geninatti Crich, S. Belfiore, L. Biancone, C. Cabella, G. Esposito, A. D. Manazza, S. Aime, *Magn. Reson. Med.* **2006**, *55*, 491–497.
- [15] U. Himmelreich, S. Aime, T. Hieronymus, C. Justicia, F. Uggeri, M. Zenke, M. Hoehn, *Neuroimage* **2006**, *32*, 1142–1149.
- [16] R. E. Eliaz, S. Nir, F. C. Szoka, Jr., *Methods Mol. Med. Methods. Enzymol.* **2004**, *387*, 16–33.
- [17] Z. Rudzki, S. Jothy, *Mol. Pathol.* **1997**, *50*, 57–71.
- [18] M. B. Herrera, B. Bussolati, S. Bruno, L. Morando, G. Mauriello-Romanazzi, F. Sanavio, I. Stamenkovic, L. Biancone, G. Camussi, *Kidney Int.* **2007**, *72*, 430–441.
- [19] A. Taglienti, F. Cellesi, V. Crescenzi, P. Sequi, M. Valentini, N. Tirelli, *Macromol. Biosci.* **2006**, *6*, 611–622.
- [20] M. R. Almofti, H. Harashima, Y. Shinohara, A. Almofti, Y. Baba, H. Kiwada, *Arch. Biochem. Biophys.* **2003**, *410*, 246–253.
- [21] L. Ciani, A. Casini, C. Gabbiani, S. Ristori, L. Messori, G. Martini, *Biophys. Chem.* **2007**, *127*, 213–220.
- [22] A. Herrera, A. Gayo, S. Jothy, *Int. J. Exp. Pathol.* **2001**, *82*, 193–200.
- [23] M. M. Knüpfner, H. Poppenborg, M. Hotfilder, K. Kühnel, J. E. A. Wolff, M. Domula, *Clin. Exp. Metastasis* **1999**, *17*, 71–76.

Received: July 17, 2008

Revised: August 27, 2008

Published online on November 5, 2008